A light Higgs particle explains physics mysteries

Stig Sundman
Dragonvägen 12 A 5, FIN-00330 Helsinki, Finland

June 27, 2016

Abstract

In a maximally simple model (MxSM), a straightforward interpretation of the Feynman diagrams for the elementary particles of the standard model (SM) suggests the existence of a close relationship between the photon, Higgs particle, neutrino, and electron. Virtual Higgs particles mediate a weak force that explains several puzzling observations in physics. Weakly interacting massive particles (WIMPs) in the form of heavy sterile neutrinos are predicted to provide the bulk of the universe's dark matter. Unlike the Higgs and neutrino, both of which may carry any mass, the related electron appears in three well-defined mass states (e, μ, and τ). MxSM, as well as minimal SM, suggest that the bulk of the mass of the electron derives from virtual photons, while a small additional mass component is generated by virtual Higgs particles, which may be looked upon as massive spin-0 photons that, unlike ordinary massless spin-1 photons, do not carry polarization.

Keywords: Maximally simple model (MxSM); pure QED; light Higgs particle; sterile neutrino; WIMP.

Contents

1 The spin-0 particle of the Feynman diagrams

1.1 The Feynman diagrams of the standard model

The solid basis of the standard model (SM) of elementary particles is provided by its well-tested Feynman diagrams and rules. Thus, in the Introduction of his book *Diagrammatica — The Path to Feynman Diagrams* [1], Martinus Veltman writes:

> "Perturbation theory means Feynman diagrams. [...] Here there is a most curious situation: the resulting machinery is far better than the originating theory."

In other words, when discussing elementary particles, one should base the reasoning on their Feynman diagrams, not on experimentally unverified theoretical speculations such as the idea that all particle masses are generated through the so-called Higgs mechanism.

In particular, one should remember that the Feynman diagrams do not specify in how many mass states an elementary particle may appear, and that the theorists were unable to predict both the existence of the heavy electron (or muon, μ) first observed in 1936 and the superheavy electron (or tauon, τ) discovered in 1975.

In Appendix E of *Diagrammatica*, Martinus Veltman summarizes the "Standard Model". In Appendix E.2 (titled "Feynman rules"), he gives a complete list of the Feynman vertices appearing in SM. In the listing there are in all 92 vertices of which 47 involve ghost particles.

> On page 249, in appendix E.1 "Lagrangian", Veltman writes: "The gauge chosen is the Feynman–'t Hooft gauge. In this gauge [...] there are ghost fields, Higgs ghosts and Faddeev–Popov ghosts. The ghost fields must be included for internal lines, but they should not occur as external lines. They do not correspond to physical particles, but they occur in the diagrams to correct violations of unitarity that would otherwise arise due to the form of the vector boson propagators chosen here. The proof of that fact is really the central part of gauge field theory."

The standard model contains seven massive elementary particles — some of them appearing in several mass states.

There exists one charged spin-1 boson, the W particle (or $W^{\pm}$). Also, there are three charged spin-$\frac{1}{2}$ fermions, namely the electron ($e^{\mp}$), the down quark (d, or $d^{\mp 1/3}$), and the up quark (u, or $u^{\pm 2/3}$), all of which also appear in a heavy and a superheavy version.

In addition to these four charged particles, there are three neutral elementary particles: the spin-1 Z boson (or Z^0), the spin-0 Higgs boson (or H), and the neutrino (ν), which is a spin-$\frac{1}{2}$ fermion.

On the next page I show the 20 basic Feynman vertices through which the seven massive particles interact with each other and with the massless photon (γ) and gluon (g^{α}, $\alpha = 1, \ldots 8$), which are polarization-carrying spin-1 bosons. The last vertex shows gluon–gluon interaction.

1.2 Feynman vertices in the standard model

The three-legged ghost-free vertices of SM are:

1	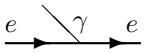	Interaction $\propto \sqrt{\alpha} \propto e$	
2	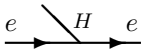	Interaction $\propto m_e$	
3	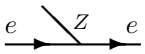		
4, 5	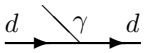	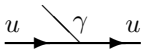	Interactions $\propto \sqrt{\alpha} \propto e$
6, 7	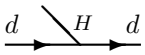	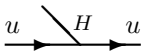	Interactions $\propto m_d,\ m_u$
8, 9	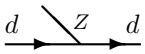	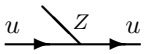	
10	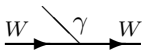		
11	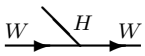		
12	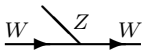		
13	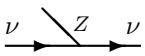		
14, 15	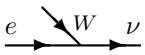	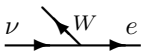	
16, 17	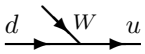	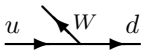	
18	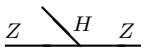		
19	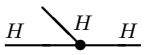	Non-perturbative for large M_H	
20, 21	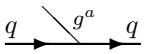	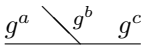	Quark–gluon, gluon–gluon interactions

Right-pointing arrows indicate particles (W^+, e^-, d, u, and ν). Similarly, left-pointing arrows are used to indicate antiparticles (W^-, e^+, $\bar{d}$, $\bar{u}$, and $\bar{\nu}$), which may be regarded as particles moving backward in time.

Note that the Higgs and Z bosons are their own antiparticles in the sense that two identical bosons may annihilate each other. Similarly the neutrino may well be its own antiparticle:

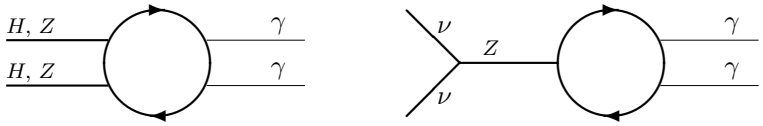

The virtual vacuum-polarization (v-p) loop in the diagrams may be formed from any charged particle and its antiparticle.

Already being pure massless radiation, the photon cannot be regarded as its own antiparticle; rather one should say that it does not have an antiparticle.

1.3 The maximum-simplicity principle (MxSP)

The term "principle of maximum simplicity" was coined by James Bjorken and Sidney Drell in 1965 when they discussed the role of simplicity as a guiding rule in the development of quantum field theory (QFT) [2]. When MxSP is applied to the minimal standard model, the result is a "maximally simple model" (MxSM).

1.4 Higgs interactions

The photon (γ) is a massless neutral spin-1 boson, while the Higgs particle (H) is a massive neutral spin-0 boson. The photon is the carrier of the electromagnetic force, while the Higgs carries a weak force. In their interaction with matter — that is, with ordinary electrons (e^-) and down and up quarks ($d^{-1/3}$ and $u^{+2/3}$) — the two particles appear in identical-looking Feynman diagrams. See Section 1.2 that begins on page 4. 4

Consider in parallel the second-order mass contributions, $\delta m^{(2)}$, to the electron from the photon and the Higgs:

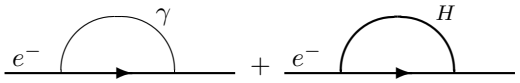

From basic electroweak theory — for instance following James Bjorken's and Sidney Drell's classical textbook "Relativisic Quantum Mechanics" (compare with Appendix B on page 35) — one obtains the expression 35

$$m = m_0 + \delta m^{(2)}(\gamma) + \delta m^{(2)}(H) = m_0 + \frac{3\alpha}{2\pi}\left(\ln\frac{\Lambda}{m}\right)\left[1 + \frac{G_F m^2}{4\sqrt{2}\pi\alpha}\right] m \qquad (1)$$

for the renormalized mass m of the electron. In the equation, m_0 is the bare mass of the electron, α the fine-structure constant, G_F the Fermi coupling constant, and Λ a cut-off mass introduced to make the mathematics finite.

In standard QED theory both m_0 and Λ tend to infinity with the result that, being the sum of two infinite terms, Eq. (1) is nonsensical. However, when MxSP is applied to it, the equation becomes meaningful. This is so because simplicity implies "pure QED", which is also referred to as "finite QED" or the "JBW hypothesis" after Kenneth Johnson, Marshal Baker, and Raymond Willey who together developed the theory in the early 1960s [3]. And, according to pure QED, the bare mass m_0 is zero.

Setting $m_0 = 0$ and ignoring contributions to m other than those shown in the figure above, one obtains from Eq. (1) the ratio

$$\frac{\delta m^{(2)}(H)}{\delta m^{(2)}(\gamma)} = \frac{G_F m^2}{4\sqrt{2}\pi\alpha} \tag{2}$$

between the two contributions to the mass of the electron.

Since the Higgs–electron diagrams exactly parallel the photon–electron diagrams (see Section 1.2), one may expect that the ratio between the Higgs and 4
photon contributions to the electron mass will remain the same as in Eq. (2) when higher-order self-mass diagrams are included in the calculation. That is, $\delta m(H)/\delta m(\gamma) = \delta m^{(2)}(H)/\delta m^{(2)}(\gamma)$ is expected to hold true.

Because Higgs and other corrections to the mass of the electron are small in comparison with the photon's contribution to it, one may set $\delta m(\gamma)$ equal to m, and obtain as a good approximation

$$\delta m(H) = \frac{G_F m^2}{4\sqrt{2}\pi\alpha} m. \tag{3}$$

Finally, resorting once again to MxSP, one may conjecture that the mass of the Higgs particle itself equals its contribution to the electron mass. That is, m_H may replace $\delta m(H)$ in Eq. (3).

> Note, however, that the relation $m_H = \delta m(H)$ was first suggested by a study of the muon–electron mass ratio [4]. Also note a suggestion that the divergent series expansions in α of perturbative QED might be replaced by convergent expansions in powers of $1/\alpha$ [5].

Therefore, using the values $1/\alpha = 137.035\ 999$ and (after restoring $\hbar$ and c, which are customarily set equal to 1) $G_F/(\hbar c)^3 = 1.166\ 36 \times 10^{-5}\ \text{GeV}^{-2}$, one obtains from Eq. (3) the relation

$$m_H = \frac{m^2}{11\ 118.8\ \text{GeV}^2} m \tag{4}$$

between the mass m of the electron and the mass m_H of the light Higgs particle that interacts with the electron.

For the mass of a Higgs particle emitted by an ordinary electron (with mass $m_e = 0.510\ 9989$ MeV), muon ($m_\mu = 105.658\ 37$ MeV), and tauon ($m_\tau = 1777$ MeV), respectively, one obtains from Eq. (4)

$$\begin{aligned} m_{H_e} &= 12.0006\ \mu\text{eV}, \\ m_{H_\mu} &= 106.085\ \text{eV}, \\ m_{H_\tau} &= 0.505\ \text{MeV}, \end{aligned} \tag{5}$$

with the masses given in electronvolts, which is customary in particle physics and simply means that c is set equal to 1 in the mass unit eV/c^2.

The self-energy $m_{H_e}c^2 = 12.0006$ μeV of the H_e particle corresponds to the energy $E_\gamma = h\nu$ of a photon of frequency $\nu = 2.9017$ GHz.

The close relationship between the photon and the Higgs, which may be regarded as a "compact photon" — a massive spin-0 variety of the ordinary massless spin-1 photon — suggests that each charged elementary particle has a Higgs particle of specific mass associated with it. Examples:

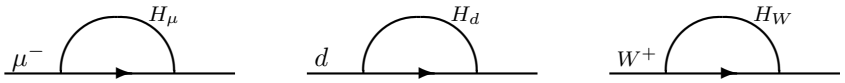

1.5 Higgs masses

There are in all 10 charged elementary particles: nine spin-$\frac{1}{2}$ fermions and one spin-1 boson, the W. To the charged elementary fermions belong the electron (e) and the down and up quarks (d and u) together with two heavier generations of each of them: muon and tauon (μ and τ) of unit charge ($\mp e$), strange and bottom (s and b) quarks with fractional charge $\mp\frac{1}{3}e$, and charm and top (c and t) quarks with fractional charge $\pm\frac{2}{3}e$.

In the case of the W boson, the Feynman rules do not suggest any specific connection between its mass, $M_W = 80.4$ GeV, and the mass M_{H_W} of the Higgs particle associated with it. However, experiments have shown it to be about $M_{H_W} = 125$ GeV.

Note that the neutral spin-1 Z boson does not couple to the photon (see Section 1.2) and therefore lacks electromagnetically generated mass. This means that its mass is of purely weak origin, generated by the H_W Higgs (right diagram above with W^+ replaced by Z).

The masses of the Higgs particle associated with the electron in its three mass states are given by Eq. (5).

In the same way as m_{H_e} is linked to m_e, the masses of the down and up-type Higgs particles (m_{H_d} and m_{H_u}) are linked to the corresponding quark masses. That is, m_d and m_u replace m_e in the expression for the Higgs–electron vertex appearing twice in the figure in Appendix B.

But what are these quark masses? The simplest assumption that results in an unambiguous prediction of their values is that the quark mass appearing in the Higgs–quark vertex is coupled to the electromagnetic mass component of the quark in the same way as the mass of the electron-type Higgs is coupled to the electron mass through Eq. (4).

If that is so, and if the electromagnetic component of the quark mass is proportional to the square of its charge, the quark masses that determine the masses of the quark-type Higgs bosons, and thereby the strength of the Higgs–

quark interactions, are

$$\begin{aligned} m_d &= \frac{1}{9} m_e, \\ m_u &= \frac{4}{9} m_e, \end{aligned} \tag{6}$$

with m_s and m_c similar fractions of m_μ, and m_b and m_t fractions of m_τ.

Since, according to Eq. (4), $m_H \propto m^3$, one has $m_{H_d} = m_{H_e}/729$ and 6
$m_{H_u} = 64\, m_{H_e}/729$. With $m_{H_e} = 12.0006$ μeV, these relations give

$$\begin{aligned} m_{H_d} &= 0.0165 \ \mu\text{eV}, \\ m_{H_u} &= 1.0535 \ \mu\text{eV}. \end{aligned} \tag{7}$$

1.6 Higgs–quark interactions

As illustrated in the figure on page 7, every charged elementary particle con- 7
stantly emits and recaptures virtual Higgs bosons possessing a mass that is specific for the particle. Thereby, the Higgs generates a "weak correction" to the mass of the charged particle. (In the case of the neutral Z boson, the Higgs generates its entire mass.)

In addition to emitting and reabsorbing Higgs particles characteristic for it, a charged particle may receive a Higgs boson of any mass and retain it for a brief moment before the law of conservation of mass forces the boson to return to the sender. The maximum time delay, Δt, between reception and emission of the Higgs is determined by the Heisenberg uncertainty relation

$$\Delta E \, \Delta t \geq \frac{1}{2} \hbar, \tag{8}$$

which in this case may be replaced by $\Delta E \, \Delta t = \hbar$ with $\Delta E = m_H c^2$. (Compare with the relation $\Gamma \tau = \hbar$, where Γ is the so-called decay width of an unstable particle and τ the lifetime of the particle. See Appendix A.) 33

1.7 The Higgs force

A comparison between the Higgs and photon Feynman diagrams suggests that the Higgs-mediated force between two charged particles is repulsive, independent of the signs of the charges, whereas the photon-mediated electromagnetic force is attractive or repulsive depending on whether the charges are of opposite or equal sign, respectively.

The fact that no repulsive electric (i.e., static) force attributable to the Higgs has been observed means that the Higgs-mediated force is of a purely dynamic nature, presumably resembling the photon-mediated magnetic force generated by an electric current flowing through a copper coil. Thus, the "magnetic Higgs force" will mainly affect particles orbiting each other at relativistic speeds.

The lowest-order diagrams for electron–electron scattering illustrate the difference between the electromagnetic force (left) and the Higgs force (middle and right with the crossing Higgs lines not touching each other):

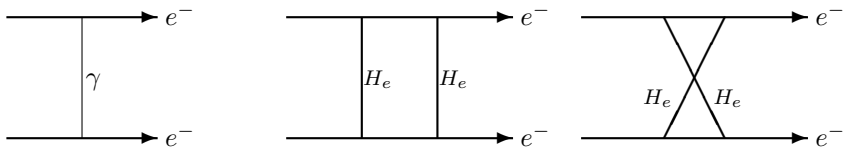

Since the law of conservation of mass forbids a permanent exchange of a single Higgs particle between two electrons, there is no Higgs parallel to the first-order photon-exchange diagram to the left in the figure.

Similarly, the repulsive quark–muon force — thought to be responsible for the proton radius discrepancy to be discussed in Section 2.4 — is described to 15
the lowest order by diagrams such as:

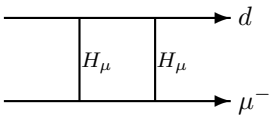

The contribution to the force deriving from a double-exchange of an H_d or H_u particle should be negligible because both H_d and H_u are much lighter than H_μ (which, according to Eq. (5) with m replaced by m_d or m_u, is true even for 6
the case that m_d and m_u are taken to be the so-called current, or bare quark masses that lie in the vicinity of 5 MeV and 2 MeV, respectively).

The repulsive force between quarks that is thought to be responsible for the "proton's missing spin" (see Section 2.2) is described to lowest order by 14
diagrams such as:

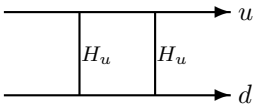

The strength of the Higgs–fermion interaction is proportional to the mass of the fermion (see vertices 2, 6, and 7 in Section 1.2). Since the lowest-order diagrams 4
describing the magnetic Higgs force between two fermions (f_1 and f_2) contain four vertices (are said to be of second order), the Higgs force is proportional to the fourth power of the mass of the fermion with which the virtual Higgs boson of the Feynman diagram is associated (say, $F_H \propto m_{f_1}^4$).

This fact suggests that the Higgs force between light and relatively slow-moving electrons is too weak to be experimentally detected. Most clearly the consequences of the repulsive magnetic force are expected to show up in protons

and neutrons in which distances are short and the quarks orbit each other at relativistic speeds.

1.8 Range of the Higgs force

An estimate of the maximum range, $r_{\max}$, of the Higgs force may be obtained from the Heisenberg uncertainty relation in Eq. (8) written in the form 8
$\Delta t = \hbar/m_H c^2$. With $r_{\max} = c\,\Delta t$, it gives

$$r_{\max} = \hbar c/m_H c^2. \tag{9}$$

For example, using $\hbar = 6.582 \times 10^{-16}$ eV s, $c = 2.998 \times 10^8$ m/s, and $m_{H_\mu} c^2 = 106.086$ eV, one obtains for the maximum range of the force mediated by a muon-type Higgs the value 0.186×10^{-8} m, or

$$r_{\max}(H_\mu) = 1.86 \text{ nm}. \tag{10}$$

1.9 Annihilation of Higgs particles

The Higgs particle is unstable and decays primarily through a virtual vacuum-polarization loop exemplified by the Feynman diagrams:

A heavy Higgs particle of mass less than $2\,M_W = 2{\times}80.4$ GeV = 161 GeV should predominantly annihilate through virtual W loops. Heavier particles would mostly decay into pairs of W bosons and, if heavier than $2\,M_Z = 2 \times 91.19$ GeV = 182 GeV, into pairs of Z bosons.

In addition to annihilating through electron loops, light Higgs particles may annihilate through quark loops.

1.10 Creation of Higgs particles

Higgs particles are mainly created in reactions opposite to the annihilation reactions — that is, in photon–photon collisions.

The corona is the hottest region of the sun with temperatures reaching about two million kelvin. This temperature corresponds to a photon energy of $E_\gamma =$ 172 eV, which follows from the relation

$$E = kT, \tag{11}$$

where $k = 8.617 \times 10^{-5}$ eV/K is the Boltzmann constant. Consequently, Higgs bosons created in photon–photon collisions in the sun form a continuous mass spectrum from well above 344 eV (say, about 10 keV) down to nearly zero.

> Two photons of energy E_γ that move in opposite directions and collide head-on may combine into a Higgs of mass $2E_\gamma$ that is at rest relative to the sun.
>
> The rest frame, or center-of-mass coordinate system, of two photons is defined as the frame in which the momenta ($\boldsymbol{p}_1$ and $\boldsymbol{p}_2$) of the photons are equaly large ($p_1 = p_2 = E_\gamma/c$) but have opposite directions ($\boldsymbol{p}_1 = -\boldsymbol{p}_2$).
>
> Consider two photons that are observed to travel in the same direction in nearly parallel trajectories. In their rest frame, the photons have momenta and energies that are nearly zero, and approach each other with the speed of light. If they collide, they may form a Higgs particle at rest with a vanishingly small mass. Seen from the perspective of the outside observer, the two photons combine into a nearly massless Higgs particle moving with practically the speed of light in the same direction as the photons did.

Another way in which Higgs particles might be produced is via neutrino–photon collisions. Thus, in the sun, H particles may be created in the process:

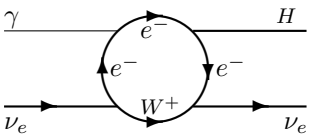

The diagram shows how an incoming electron-type neutrino produced in the core of the sun splits into a particle pair ($\nu_e \rightarrow e^- + W^+$), after which the virtual electron absorbs an incoming photon and emits a Higgs particle before it rejoins the W^+ particle, and together with it forms an outgoing neutrino.

Because the electron-type neutrinos that are created in nuclear reactions in the sun oscillate into both muon and tauon-type neutrinos, similar reactions occur in which the ν_e neutrino is replaced by a ν_μ or ν_τ neutrino.

1.11 Higgs lifetimes

Heavy Higgs particles have very short lifetimes. An attempt to estimate the lifetimes of very light Higgs particles annihilating through virtual electron loops (see Appendix A) suggests that their lifetimes are proportional to the Higgs 33
mass. For the H_e particle of mass 12 μeV annihilating via en electron loop, the result is 34

$$\tau_{H_e}(e) = 2.37 \times 10^8 \text{ s} = 7.5 \text{ yr}. \tag{12}$$

The rest energy, 12 μeV = 0.012 meV of this particle is much lower than the energy $E = kT = 0.0253$ eV = 25.3 meV of particles at room temperature 10
(20 °C = 293.15 K).

The particle's rest energy corresponds to the energy of a thermal photon at temperature $(0.012/25.3) \times 293.15$ K = 0.14 K. Therefore, the H_e particle will always be moving at speeds very close to the speed of light, and consequently have an effective lifetime much longer than 7.5 years.

Even a million times heavier Higgs particles (with a mass of 12 eV and a lifetime at rest of $2.37 \times 10^8/10^6$ s = 237 s, or about 4 minutes) might live long enough in the corona for a considerable part of them to escape out into space and occasionally hit a planet.

1.12 Higgs in beta-decay and electron-capture processes

In addition to decaying spontaneously, Higgs particles may end their lives in beta-decay and electron-capture processes, which normally proceed in the manner shown in the figure:

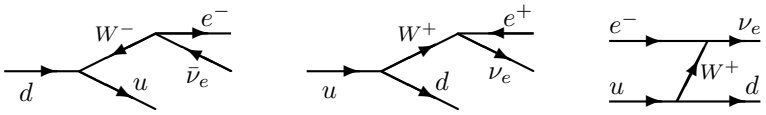

The left diagram illustrates negative beta decay through which a neutron (udd) transforms into a proton (uud), an electron (or β^- particle), and an antineutrino.

The diagram in the middle illustrates positive beta decay through which a proton transforms into a neutron, an antielectron (i.e., a positron, or β^+ particle), and a neutrino.

The diagram to the right shows electron capture — the process through which a proton transforms into a neutron by capturing an electron and emitting a neutrino. In the figure, a W^+ particle emitted by one of the proton's two u quarks is absorbed by the electron being captured. Alternatively, a W^- particle emitted by the electron may be absorbed by one of the u quarks.

In all three types of weak decay, a free Higgs particle may in theory trigger the reaction, thereby accelerating the decay rate:

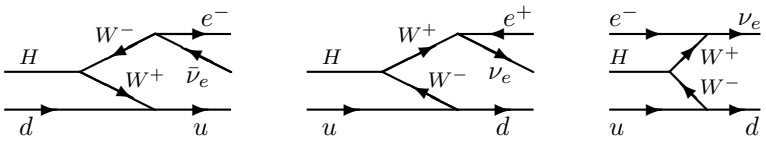

2 Possible observations of virtual Higgs bosons

In the same way as virtual photons mediate the electromagnetic force, virtual Higgs particles mediate a weak force. As a result, the light virtual Higgs particles manifest their presence in many ways.

2.1 The muon ($g - 2$) experiment

In the most expensive experiment in high-energy physics hitherto completed — the "muon ($g - 2$) experiment" at Brookhaven [6] — physicists measured

the muon's anomalous magnetic moment (a_μ), which is half of its $g-2$: $a_\mu = (g_\mu - 2)/2$, where g_μ designates the gyromagnetic factor of the muon.

> The planning of the experiment began before the previous series of measurements, which took place in the years 1974 to 1976, had finished. Construction of the necessary requisites (including cyclotron, magnetic storage ring, measuring instruments, and other peripheral equipment) took a long time. The measurements were performed during the years 1997 to 2001, and after five separate reports had been published, the *"Final Report of the Muon E821 Anomalous Magnetic Moment Measurement at BNL"* appeared in 2006.

The diagram in the figure shows the Higgs particle's contribution to the anomalous magnetic moment of the muon:

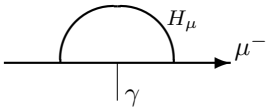

In the same way as Eq. (3) for the contribution of the Higgs particle to the electron mass is derived from basic electroweak theory, an elementary calculation of the Higgs particle's contribution to a_μ gives the value 6

$$a_\mu(H_\mu) = \frac{3G_F m_\mu^2}{8\sqrt{2}\pi^2} = 0.000\ 000\ 003\ 50 \quad (m_{H_\mu} \ll m_\mu) \tag{13}$$

in the case where the mass m_{H_μ} of the Higgs particle (H_μ) appearing in the diagram tends to zero. The general expression, which holds for all values of m_{H_μ}, shows that the contribution is vanishingly small when $m_{H_\mu} \gg m_\mu$.

The sum of the contributions to a_μ from the rest of the elementary particles of SM is found to be

$$a_\mu^{\text{th}}(\text{SM}) = 0.001\ 165\ 917\ 78(61), \tag{14}$$

which means that the total theoretical value is

$$a_\mu^{\text{th}} = 0.001\ 165\ 921\ 28(61) \quad (m_{H_\mu} \ll m_\mu) \tag{15}$$

and

$$a_\mu^{\text{th}} = 0.001\ 165\ 917\ 78(61) \quad (m_{H_\mu} \gg m_\mu), \tag{16}$$

respectively, in the two cases. The value obtained in the experiment was [7]

$$a_\mu^{\text{exp}} = 0.001\ 165\ 920\ 91(63). \tag{17}$$

Thus, its deviation from the theoretical value in Eq. (15),

$$a_\mu^{\text{exp}} - a_\mu^{\text{th}} = -0.000\ 000\ 000\ 37(88) \quad (m_{H_\mu} \ll m_\mu), \tag{18}$$

is well within the margin of error (note that the uncertainties are added in square: $61^2 + 63^2 = 88^2$), which indicates good agreement between theory and observation. In contrast, its deviation from the value in Eq. (16),

$$a_\mu^{\text{exp}} - a_\mu^{\text{th}} = +0.000\ 000\ 003\ 13(88) \quad (m_{H_\mu} \gg m_\mu), \tag{19}$$

indicates a discrepancy between theory and observation of $313/88 = 3.5$ times the error margin.

In summary, comparison of the experimental and theoretical values of a_μ suggests that the Higgs particle (H_μ) associated with the muon has a mass that lies considerably below the muon mass, $m_\mu = 105.66$ MeV. Therefore, H_μ cannot possibly be identical to the heavy Higgs particle with a mass of about 125 GeV.

> If the muon $(g-2)$ experiment had been an "ordinary" experiment, one could have dismissed the result by explaining that the large discrepancy for a heavy Higgs might well result from undetected experimental or theoretical errors. But, since it doubtless was up to then the world's most thoroughly analyzed experiment — just as the computations of a_e and a_μ are by far the most thoroughgoing theoretical determinations of physical constants ever done — the result is believed to be very solid.
>
> This conclusion is underpinned by the observation that a refined analysis made after the final report was published in 2006 didn't result in a diminishing, but in an increasing discrepancy for $m_{H_\mu} \gg m_\mu$; that is, from $+0.000\ 000\ 003\ 02(88)$ in 2008 to $+0.000\ 000\ 003\ 13(88)$ in 2010.

It may be mentioned that the measured value of the ordinary electron's anomalous magnetic moment, $a_e^{\text{exp}} = 0.001\ 159\ 652\ 180\ 73(28)$, has an accuracy that is 2000 times higher than the accuracy of the experimental value of a_μ. But, since the contribution $a_e(H_e) = 3G_F m_e^2/8\sqrt{2}\pi^2$ is $(m_\mu/m_e)^2 = 206.768^2 \approx 40\ 000$ times less than $a_\mu(H_\mu)$, the value of a_e still isn't precise enough to give any further information about the mass of the light Higgs particle.

2.2 The proton's missing spin

In nuclear physics, there are a number of puzzling observations, which might be explained by the existence of a very light Higgs particle that produces a force of sufficiently long range to affect the behavior of the constituent particles (the down and up quarks) of the nucleons. One of these effects is "the proton's missing spin".

The proton's spin is the sum of the orbital and spin angular momenta of its constituent particles (quarks and gluons). However, experiments indicate a gap between the proton's spin angular momentum of $\frac{1}{2}\hbar$ and the sum of its component particles' theoretically estimated orbital angular momenta and observed spin angular momenta [8]. A Higgs force affecting the dynamics of the quarks might explain the discrepancy.

Asymptotic freedom implies that the strong force that glues quarks together vanishes for $r \ll r_p$, where r is the distance between the quarks and r_p the proton radius. The figure shows the quarks of the proton positioned on a common line with the down quark of fractional charge $-\frac{1}{3}e$ at the center:

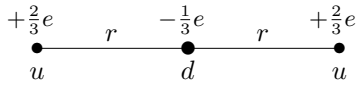

The electric force between one of the up quarks and the down quark is attractive and proportional to $-(+\frac{2}{3}e)(-\frac{1}{3}e)r^{-2} = +\frac{2}{9}e^2r^{-2}$, where e is the unit charge. The corresponding force between the two up quarks is repulsive and proportional to $-(+\frac{2}{3}e)^2(2r)^{-2} = -\frac{1}{9}e^2r^{-2}$. The positive sum, $+\frac{2}{9}e^2r^{-2} - \frac{1}{9}e^2r^{-2} = +\frac{1}{9}e^2r^{-2}$, suggests that there is a net inward force acting on the quarks even when r is small and the strong force negligible. Consequently, the three quarks tend to stick closely together at the center of the proton, which means that their orbital angular momenta are small.

The situation changes radically if a repulsive Higgs force outweighs the attractive electromagnetic force and causes the quarks to move in orbits as wide as allowed by the strong force (which, like the force of a rubber band, increases with increasing r). Therefore, if virtual lightweight Higgs particles are present, the angular momenta of the quarks might be considerably larger than they would be if the Higgs particles were absent.

Consequently, the existence of light scalar Higgs bosons provides a simple explanation for the proton's missing-spin mystery within the framework of SM.

2.3 The nucleons' magnetic moment

The theoretically predicted values for the magnetic moments of the nucleons (proton and neutron) and other hadrons tend to be considerably smaller than the experimentally observed values [9].

The same effect that explains the "proton spin crisis" — why the sum of the quarks' theoretically calculated spatial angular momenta, the experimentally determined quark spin angular momenta, and the estimated net glue polarization is less than the proton's spin — should explain why the magnetic moments of hadrons are larger than theoretical considerations suggest they should be.

2.4 The proton radius

Another problem in nuclear physics is that measurements of the proton radius using muonic hydrogen (where the electron that orbits the proton is replaced by a muon) and ordinary hydrogen yield nonmatching results: $r_p = 0.841\,84(67)$ fm and 0.8768(69) fm, respectively [10].

The straightforward explanation for the difference of 0.035(7) femtometer is that the light muon-type Higgs, whose existence the Brookhaven muon $g - 2$

experiment convincingly demonstrates (see Section 2.1), causes a repulsive force between the quarks of the proton and the muon orbiting it. 12

The "Bohr radius" of the hydrogen atom is $a_0 = 52\ 918$ fm. For a proton circled by a muon, the corresponding radius is smaller by a factor of m_μ/m_e. That is, $a = a_0/206.768 = 256$ fm for muonic hydrogen atoms. This distance is well within the estimated maximum range of the H_μ-mediated force, which according to Eq. (10) is $r_{\max}(H_\mu) = 1.86$ nm $= 1860\ 000$ fm. 10

2.5 The Hoyle state

A puzzle that emerged some 60 years ago is the so-called Hoyle state, which current models of atomic nuclei are unable to explain. It relates to the fusion in stars of light elements into successively heavier elements — up to iron, which is element number 26 ($_{26}$Fe) and the heaviest element that can be produced in a stellar fusion process that yields more energy than it consumes. The mystery is how stable carbon, $^{12}_{6}$C, an element that is crucial for life to form, can be produced in large amounts in the stars.

The sun is a nuclear reactor in which four protons, or hydrogen nuclei ($^{1}_{1}$H), fuse into an *alpha particle*, or helium nucleus ($^{4}_{2}$He). In the process, two of the protons transform to neutrons via absorption of an electron (e^-) or emission of a positron (e^+). When its hydrogen supply eventually runs short, the sun will become a *red giant*, whose energy is produced via the combination of two alpha particles (or helium-4 nuclei) into an unstable $^{8}_{4}$Be isotope (beryllium's stable isotope is $^{9}_{4}$Be). The fusion of an $^{8}_{4}$B and a $^{4}_{2}$He nucleus produces in turn the stable carbon nucleus $^{12}_{6}$C. And it's the efficiency of this process that puzzles physicists.

During its short lifetime — about 10^{-16} seconds or less (depending on its mode of decay) — the beryllium isotope will in general not have time to fuse with a helium nucleus and form a stable carbon nucleus ($^{8}_{4}\mathrm{B} + {}^{4}_{2}\mathrm{He} \rightarrow {}^{12}_{6}\mathrm{C}$). Instead, stable carbon is produced in red giants via an intermediate state, the *Hoyle state*, which is a short-lived excited form of the carbon nucleus C-12.

A recently performed *ab initio* lattice calculation [11] of the ground and Hoyle states of carbon-12 demonstrates that the carbon nucleus in its stable state exhibits a compact triangular configuration of three alpha particles (to the left in the figure), while in its unstable and highly dynamical state it also appears in an elongated "bent-arm configuration" (to the right):

The existence of the elongated state suggests that a repulsive dynamic force of longer range than the attractive strong force tends to prevent the three alpha particles from immediately forming a compact triangular formation.

> The strong force attempts to gather the alpha particles as close to each other as possible. It is counteracted by the repulsive electrostatic force between the positively charged alpha particles. If these two well-known forces were the only forces acting in atomic nuclei, the process should be relatively easy to calculate. The fact that, after 60 years of effort, physicists still aren't able to understand the Hoyle state with its complex dynamics (for instance, evidence is found for a "low-lying spin-2 excitation of the Hoyle state" [11]) suggests that a third force plays a critical role in the formation and maintenance of the state.

The logical conclusion is that the light Higgs particle mediates a dynamic force that should be able to explain the formation and properties of the excited Hoyle state.

2.6 The flyby anomaly

The so-called flyby anomaly is a puzzling effect observed when spacecraft destined for the outskirts of our planetary system pass near the earth to change their trajectories. It manifests itself as a mysterious acceleration of the spacecraft that varies in magnitude from one flyby to another.

As far as I understand, satellites moving in eccentric orbits and repeatedly passing close to the earth do not experience similar effects. Therefore, my conclusion is that the anomalous acceleration isn't a real effect, but is caused by errors in the measurements of the position of the spacecraft.

In communication with the spacecraft, the S band between 2 and 4 GHz is used. For instance, Pioneer 10 and Pioneer 11 transmitted on frequency 2.29 GHz. Therefore, a possible explanation for the measurement error might be that radio signals of frequencies in the vicinity of 3 GHz experience an anomalous retardation when they travel through the interplanetary plasma.

Now, the Higgs particle H_e associated with the electron is predicted to have a mass (or self-energy) that corresponds to the energy of a photon with frequency 2.9017 GHz. See paragraph after Eq. (5). This means that a radio signal of 6
frequency near 2.9 GHz, which travels through a medium, by necessity will experience a *Higgs delay* in addition to the well-known delay resulting from the photon's electromagnetic interaction with the medium.

> A photon traveling through empty space oscillates between various states. In addition to forming a single-photon state, it may form a virtual particle pair consisting of any charged elementary particle and its antiparticle (a so-called *vacuum-polarization (v-p) loop*). The figure shows two examples of v-p loops:
>
> 
>
>
> The virtual massive particles appearing in the photon propagator do not slow down the speed of a free photon, which in vacuum travels at the speed of light, c.

The larger the difference between the photon's energy (E_γ) and the rest energy ($2mc^2$) of the particle pair, the shorter the time the photon may remain in the particle–antiparticle state.

Through mediation of polarization loops, the photon may momentarily transform into a photon triplet or a Higgs–photon pair (but, according to the Furry theorem, not a pair of photons):

The lifetime of the Higgs–photon state depends on the ratio between the photon's energy (E_γ) and the Higgs particle's rest energy ($m_H c^2$). The closer these energies are to each other, the longer the lifetime of the Higgs–photon pair will be. And the longer it exists, the higher the probability that the pair will hit an electron or other charged particle in the medium.

The next figure shows examples of electromagnetic delay (left) and Higgs delay (right) of light in a medium:

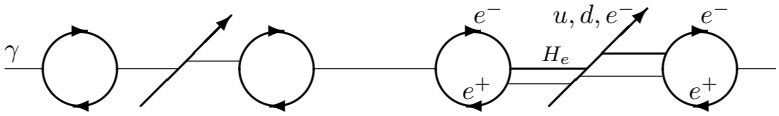

Both types of delay are different in the lower layers of the atmosphere, in the ionosphere with its free electrons, and in the Van Allen belts with their accumulations of hydrogen plasma in the form of free protons and electrons in equal amounts.

So, why hasn't any anomalous Higgs delay been observed in communications with satellites orbiting the earth? I guess the answer is that the global positioning system (GPS) being used is constantly calibrating itself using algorithms that are unable to distinguish a small Higgs delay from the much larger electromagnetic delay. Also, in comparison with the electromagnetic delay, the Higgs delay may well be too small to be discernible except for signals traveling through the hydrogen plasma filling interplanetary space and being amassed in the Van Allen belts.

In the lower atmosphere, as well as in the ionosphere located at an altitude of about 50 to 1000 km, the atomic nuclei of mainly nitrogen and oxygen molecules are shielded by electron shells, which prevent the electromagnetically interacting photons from reaching the fractionally charged quarks of the nucleons.

In a signal arriving from a passing spacecraft, an anomalous Higgs delay is expected to show up when the signal traverses regions containing relatively dense hydrogen plasma; that is, the inner and outer Van Allen belts at altitudes of about 1000 to 10 000 km and 15 000 to 25 000 km, respectively.

Depending on the direction of motion of these plasma belts relative to the radio signal, the magnitude of the anomalous Higgs delay may vary greatly.

Seen from an approaching spacecraft, the Van Allen belts are rocking up and down as the earth rotates around its axis.

> The Van Allen radiation belts form a circular, doughnut-shaped zone stretching around the magnetic equator — that is, symmetrically around the axis that joins the magnetic North Pole with the magnetic South Pole. The fact that this axis is inclined some 20 degrees (the inclination varies with time) relative to the earth's axis of rotation means that, seen from an approaching spacecraft, the radiation belts rock up and down as the earth rotates around its axis. To visualize this movement of the Van Allen belts, I draw a figure:

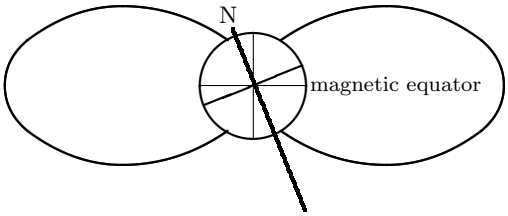

> In the figure, the vertical axis connects the magnetic poles of the earth with each other. The thick oblique line indicates the axis of rotation of the earth. I imagine it as a stick I hold in my hands. By figuring that I rotate it 180 degrees, I can imagine how a distant observer sees the magnetic belts move up and down in a half day.
>
> My conclusion is that various spacecraft exhibit seemingly random flyby anomalies depending on the position of the Van Allen belts when the spacecraft reach their perigee — the point of the orbit closest to the earth.

The plasma belts will not only affect the distance measurements (the ranging data). The motion of the belts will also give rise to a transverse effect by causing the signal to drift sideways in a manner that depends on the position of the approaching spacecraft, the position of the receiving radio station and the time of day (whether the Van Allen belts are moving up or down). Another cause of signal drift is the solar wind (the motion of protons and electrons away from the sun).

Naturally, all these effects are taken into account in the determination of the position of the spacecraft. However, what remains unaccounted for is the additional delay of the signal with accompanying sideway drift that results from the virtual Higgs particle's collisions with quarks in the plasma's protons and neutrons (which should exist in small numbers in deuterium and hydrogen nuclei appearing in the solar wind).

In summary, taking the Feynman diagrams for the photon and Higgs particles at face value leads to the prediction that a weakly interacting spinless (or polarization-free) photon with rest energy equaling the energy of an ordinary photon with frequency 2.90 GHz is associated with the electron (e). The

existence of this H_e particle means in turn that an anomalous (that is, unanticipated) delay of microwaves at frequencies near 2.90 GHz occurs.

Finally, if the magnitude of this unexpected delay is sufficiently large, it will by necessity lead to an apparently anomalous behavior of spacecraft that sometimes pass as near as 500 km from the earth — compare with the earth's radius of nearly 6400 km. Spacecraft passing still closer to the earth are affected by atmospheric drag which masks their anomalous acceleration.

With access to all the data about the flybys, it should be a straightforward task to check whether the suggested explanation is plausible or not.

2.7 The Pioneer anomaly

The Higgs delay assumed to be responsible for the flyby anomaly should cause an effect similar to the so-called Pioneer anomaly [12], which puzzled physicists for twenty years.

> Pioneer 10 was launched in 1972 and Pioneer 11 in 1973. When the two spacecraft — after fulfilling their main mission: encounters with Jupiter and Saturn — were leaving the solar system in the early 1980s, measurements indicated that they were slightly less far from the sun and the earth than calculations suggested they should be. This discrepancy between theory and observation seemed to be caused by a mysterious acceleration of the spacecraft toward the sun.

Although a recent study has concluded that the anomalous acceleration of the Pioneer 10 and 11 spacecraft is caused by "anisotropic emission of thermal radiation off the vehicles" [13], it does not exclude that a small part of the anomaly might be due to the appearance of H_e particles, which give rise to a small additional delay of the spacecraft radio signals as they travel through the interplanetary plasma.

In other words, taking the Feynman diagrams at face value led to an earlier postdiction, which in the light of a more recent study has transformed into an experimentally testable prediction:

Pioneer 10 and 11 transmitted on frequency 2.29 GHz [12], only 21 % below the 2.90 GHz corresponding to the H_e mass. The measuring systems were 7
calibrated when the spacecraft were in the vicinity of the earth. Due to the unrecognized Higgs delay, the radio signals traveled slightly slower than they were expected to. Therefore, as the spacecraft approached the outer edge of the solar system and the plasma became thinner, signal speed increased more than it was expected to — that is, more than it would have increased if the delay had been caused solely by absorption and reemission of the radio signal's photons. The result was that the signals arrived earlier than anticipated, and the spacecraft appeared to be nearer to the sun than they actually were.

3 Possible observations of real Higgs bosons

3.1 The sun's hot corona

The sun's atmosphere consists of the photosphere hundreds of kilometers thick with an average temperature T of 5780 K, the chromosphere about 10 000 km thick with T rising from about 4000 K to about 50 000 K, and the corona with T reaching about two million K at a height of some 75 000 km [14].

The high temperature of the corona has mystified astrophysicists, and no convincing explanation for it has been found.

> In want of a simple explanation, it has been suggested that the corona's high temperature is caused by hypothetical so-called nanoflares, which are too small to be individually detected, and with an underlying mechanism that is not known [15].

The presence of light Higgs particles might present a solution to the mystery. Solar neutrinos created in boron decay, ${}^{8}_{5}\mathrm{B} \rightarrow {}^{8}_{4}\mathrm{Be}^{*} + e^{+} + \nu_e$, acquire energies approaching 14 MeV [16, p. 452]. Consequently, energetic Higgs particles may be produced in considerable numbers in the corona. Before and after their annihilation into photons, they will give off their excess energies to the surrounding plasma.

From Eq. (11) one finds that 10 MeV corresponds to a temperature of 10
$T_\gamma = 10\ \mathrm{MeV}/8.617 \times 10^{-5}\ \mathrm{eV/K} = 116\ \mathrm{GK}$ (116 billion kelvin). This is 58 000 times higher than the typical maximum temperature 2 MK of the corona. Consequently, a single Higgs particle may heat about 60 000 photons from a few thousand kelvin to 2 MK.

Naturally, the local temperature of the corona depends on its matter density and how quickly the existing coronal matter is replaced with new matter transported by large solar flares.

Still, it should be a fairly easy task to calculate the amount of energetic Higgs particles produced in the sun's atmosphere, and estimate how much they heat the corona.

3.2 The tritium endpoint anomaly

Beta decay of tritium means that a radioactive hydrogen atom, with one proton and two neutrons in its nucleus (${}^{3}_{1}\mathrm{H}$, or tritium), decays into a helium-3 atom (${}^{3}_{2}\mathrm{He}$) with two protons and one neutron in its nucleus at the same time as a beta particle (e^{-}) and an antineutrino ($\bar{\nu}_e$) are emitted: ${}^{3}_{1}\mathrm{H} \rightarrow {}^{3}_{2}\mathrm{He} + e^{-} + \bar{\nu}_e$.

When physicists began to suspect that the mass of the neutrino is not zero, which it originally was assumed to be, they tried to determine the mass m_{ν_e} of the electron neutrino by measuring the energy of the outgoing electron and subtracting from it the radiation energy known to be released in a spontaneous decay of the tritium nucleus. A negative difference even in the limit of zero kinetic energy ($v_{\nu_e} = 0$) of the neutrino would indicate that the neutrino has nonzero mass.

> The radiation energy produced in the decay is the sum of the total (kinetic plus rest) energy (E_e) of the electron and the corresponding, unobservable, neutrino energy (E_ν). Let ΔE be the difference between the experimentally obtained electron energy E_e and the theoretically calculated sum, $E_e + E_\nu$. Since the neutrino possesses mass, this difference is always negative: $\Delta E = E_e^{\text{exp}} - (E_e + E_\nu)^{\text{th}} \leq -m_\nu c^2$. Thus, in the limit of zero kinetic neutrino energy, the energy difference should approach a maximum value of $\Delta E = -E_\nu^{\text{min}} = -m_\nu c^2$.

Against all expectations, the maximum difference proved to be neither negative nor zero, but positive. No explanation was found for this phenomenon, which was dubbed "the tritium endpoint anomaly". The possibility that the mysterious extra energy might derive from neutrinos captured by the tritium nuclei was soon ruled out.

An explanation of the phenomenon might be that Higgs particles with a comparatively long lifetime — that is, light particles traveling with relativistic speeds — are produced in the sun and reach the earth, where they occasionally trigger beta decay through the mechanism suggested in Section 1.12 (bottom figure, left diagram). This means that the observed additional energy is supplied by Higgs particles that are even more difficult to study than neutrinos. 12

Note, however, that the tritium endpoint anomaly may have a more prosaic explanation. See question at the end of Section 3.4.

3.3 Seasonal variations in radioactive half-lives

For a long time, it was taken as an established fact that radioactive decay rates are constant.

Later, the validity of this assumption was questioned. A number of observations were interpreted to indicate that the half-lives of beta-decaying radionuclides exhibit seasonal variations [17, 18].

However, more recent experiments [19] claim to disprove the existence of seasonal variations in decay rates.

Still, it cannot be excluded that light Higgs particles arriving from the sun might accelerate beta-decay of some radionuclides. Compare with Sections 1.12 and 3.2. If that is so, seasonal variations in the sun–earth distance should lead to variations in the decay rates of those nuclides. 12 21

Whether the variations are large enough to be experimentally detectable is another question.

3.4 The neutron lifetime discrepancy

The neutron is a beta-decaying particle ($n \to p + e^- + \bar{\nu}_e$) with a presumably constant half-life. Still, measurements of the neutron's lifetime (τ_n) using the beam method and the bottle method give different results. The difference is reported to be $\Delta\tau_n = \tau_n^{\text{beam}} - \tau_n^{\text{bottle}} = (888.0 \pm 2.1)\ \text{s} - (879.6 \pm 0.8)\ \text{s} = (8.4 \pm 2.2)\ \text{s}$, which implies a 3.8σ discrepancy between the two results [20].

Beam experiments are performed in laboratories at room temperature. In bottle experiments ultracold neutrons (UCNs) are used. Consequently, in laboratories performing bottle experiments, there is cold matter present. For instance, liquid deuterium may be used to first cool the neutrons from room temperature to about 25 K. This fact might be taken to indicate that cold light Higgs particles present in laboratories performing bottle experiments are responsible for the accelerated decay of the neutrons. If that is so, it means that the probability for Higgs particles to trigger beta decay increases with decreasing Higgs energy.

This idea sounds plausible, and suggests that the acceleration of neutron decay reaches its maximum at ambient temperatures somewhere between zero kelvin and room temperature.

But there is a problem with the explanation: to be able to reach the earth in appreciable numbers, the Higgs particles triggering the decay would have to be very light. This light mass means that, even at very low temperatures, they would travel at relativistic speeds with correspondingly long mean free paths, which would prevent any noticeable cooling within the limited amount of "cryonic matter" present in the vicinity of the bottle containing the ultracold neutrons.

However, there exists a simple alternative explanation illustrated by the figure:

The left diagram shows what happens when a neutron (ddu) spontaneously decays into a proton (duu), an electron, and an electron antineutrino. The right diagram shows the same decay triggered, not by a nearly massless Higgs boson, but by a photon.

Unlike Higgs particles, photons have very short mean free paths in ordinary matter. This means that photons hitting the neutrons in the bottle experiment should have the same temperature as the inner wall of the bottle.

But, if thermal photons may trigger neutron decay, shouldn't they also affect the rate of decay of radionuclides? No, the electrons orbiting atomic nuclei shield them from being hit by low-energy photons. Only free neutrons lack a shielding electron shell.

The existence of light Higgs particles in sufficient numbers to measurably trigger beta decay may be doubted. But the abundant presence of thermal photons is an undeniable fact. Therefore, the conclusion can only be that if accelerated neutron decay really occurs, it is primarily caused by thermal photons, with the contribution from Higgs bosons to the effect possibly not discernible.

One might suspect that only photons possessing a certain, rather precise energy are able to trigger neutron decay. If that is so, and if the "resonance energy" corresponds to a temperature not very far below room temperature, it might be possible to determine it via repeated beam experiments performed

"outdoors" at places with large temperature fluctuations between day and night and between summer and winter.

> Could it also be that the tritium endpoint anomaly discussed in Section 3.2 is mainly caused by photons? It seems plausible that the single electron in the shell of the tritium atom cannot entirely prevent the two neutrons of its nucleus from being hit by thermal photons arriving from all directions. Since the lifetime of the neutron seems to vary with the temperature of the thermal photons hitting it, one may expect the magnitude of the tritium endpoint anomaly to vary with the temperature at which the experiment is performed. 21

3.5 The lithium problem

In the hot interior of stars, lithium is burned to helium through fusion with a proton ($^7_3\mathrm{Li} + p \rightarrow {}^8_4\mathrm{Be} + 17.3$ MeV) followed by fission of the resulting beryllium nucleus ($^8_4\mathrm{Be} \rightarrow {}^4_2\mathrm{He} + {}^4_2\mathrm{He} + 92$ keV). Proton–lithium fusion requires a temperature of approximately 2×10^6 K, which is less than the 2.5×10^6 K necessary for hydrogen fusion. However, only protons possessing energies much higher than their average energy are able to overcome the Coulomb barrier and fuse with lithium nuclei.

With a lifetime of about 7×10^{-17} s, the beryllium-8 nucleus almost instantly splits into two helium nuclei (or alpha particles), each one carrying about 8.6 MeV of kinetic energy.

The amount of lithium-7 believed to have been created in the primordial nucleosynthesis matches the amount observed in the Small Magellanic Cloud [21].

However, in the atmospheres of old, so-called galactic halo stars, there is about one fourth as much lithium-7 as predicted [21].

A possible explanation for this mismatch between theory and observation is supplied by the light Higgs particle, which suggests a mechanism through which solar neutrinos may cause lithium depletion. That is, in a collision with a proton, a high-energy Higgs may heat the proton to a temperature that enables it to fuse with a lithium-7 nucleus.

An experiment performed in 1932 demonstrated that, for a proton to be able to overcome (or tunnel through) the Coulomb barrier and fuse with a lithium-7 nucleus, it requires an energy of about 0.1 MeV [22]. This energy is several hundred times higher than the energy $E = kT = 170$ eV corresponding to the temperature $T = 2{\times}10^6$ K. (The average kinetic energy of a *thermal neutron* [23] is $\frac{3}{2}kT$, its most probable kinetic energy is $\frac{1}{2}kT$, and its most probable speed $v = (2kT/m)^{1/2}$; that is, a thermal particle with kinetic energy $\frac{1}{2}mv^2 = kT$ moves with the most probable speed.)

Solar neutrinos created in boron decay may acquire energies that approach 14 MeV [16, p. 452]. In a $\nu\gamma \rightarrow \nu H$ reaction, the neutrino may give over most of its energy to the Higgs it creates from a photon. For simplicity, assume that the Higgs gets an energy of 9.38 MeV, which is one percent of the proton's rest energy. According to Eq. (20) below, it means that $\Delta E/E = 0.02$. In other words, the proton may acquire two percent of the energy of the Higgs particle, 21

or 0.19 MeV, which is more than the mentioned 0.1 MeV it needs to fuse with a lithium nucleus. It follows that a single Higgs with an initial energy about or above 10 MeV may heat dozens of protons to 0.1 MeV.

> The massless photon's energy E is connected to its momentum p via the relation $E = pc$. The same relation holds approximately for a relativistic particle with energy $E \gg mc^2$. Conservation of momentum in the light Higgs particle's elastic head-on collision with a proton at rest means that the Higgs reverses its direction and that, consequently, $p = -(p - \Delta p) + Mv$, where M is the mass of the proton and v its speed. For the light Higgs (compare with a light ping-pong ball hitting a heavy solid iron ball), its loss of momentum, Δp, may be ignored. Thus, $p = -p + Mv$, or $Mv = 2p = 2E/c$. That is, the maximum energy passed to the proton is $\Delta E = \frac{1}{2}Mv^2 = \frac{1}{2}(Mv)^2/M = 2p^2/M = 2E^2/Mc^2$, and
>
> $$\Delta E/E = 2E/Mc^2. \tag{20}$$

3.6 A 750-GeV Higgs particle

On 15 December 2015, a surprising discovery was announced. A 750-GeV boson, six times heavier than the 125-GeV Higgs boson observed a few years earlier, had very likely been observed through its decay into a pair of photons, a so-called diphoton.

Since MxSM allows Higgs particles of any mass to exist, the observation may have a simple explanation: in the experiment, a tetraquark consisting of two top–antitop pairs is occasionally produced. It rapidly decays into a pair of gluons ($t\bar{t}\ t\bar{t} \to gg$), which through a virtual quark loop decays into a Higgs particle:

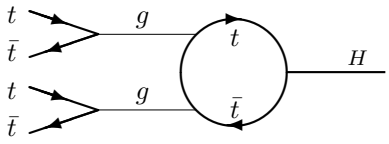

Next, the Higgs annihilates into a pair of photons through a virtual W or fermion (most likely, top) loop.

Note that the value 750 GeV/4 = 187.5 GeV agrees with the mass of the top quark whose measured value is reported to lie in the vicinity of 186 GeV.

If the explanation is correct, one should expect similar bumps to show up near 17 GeV and 5 GeV, which — since the masses of the bottom and charm quarks are around 4.3 GeV and 1.3 GeV, respectively — should be the approximate energies of the $b\bar{b}\,b\bar{b}$ and $c\bar{c}\,c\bar{c}$ tetraquarks.

So, why haven't such bumps been reported? Is it that they do not exist? Or could it be that they haven't been searched for? Or, are they indistinguishable from the background?

3.7 Dark matter

Observations of the motion of stars in the Milky Way and other galaxies suggest that the universe contains considerable amounts of so-called missing mass, or dark matter.

The lifetime of the Higgs tends to infinity ($\tau_H \to \infty$) as its mass approaches zero ($m_H \to 0$). This fact suggests that very light Higgs particles form invisible, long-lived dark matter. These practically massless and highly relativistic particles are expected to behave like indestructible photons in thermal balance with the surrounding matter. Therefore, they may appreciately contribute to the "dark matter" of galaxies.

In MxSM, as well as in minimal SM, there is only one particle that is stable, massive, and invisible. This is the so-called sterile neutrino that does not interact with ordinary matter.

> Neutrinos may be created in two types of processes; from an electron through the reaction $e^- + W^+ \to \nu$ and from a Z particle via $Z \to \nu\bar{\nu}$ (see vertices 14 and 13, respectively in Section 1.2). 4
> Radioactive decay of matter takes place through the former reaction and produces compound neutrinos able to interact with all three electrons (e, μ, and τ). In contrast, the mass of neutrinos produced from decaying Z particles is not constrained in any way. Therefore, these "sterile" neutrinos are expected to exist in a continuous mass spectrum.

Consequently, the sterile neutrino is a likely candidate for the dark matter, whose existence is inferred from its gravitational effects.

The observed photon–baryon number ratio is $N_\gamma/N_b \approx 1.65 \times 10^9$. That is, there are more than a billion photons per baryon (proton or neutron) in the universe.

In the immense heat of the early universe, photons in head-on collisions produced very heavy Z particles that sometimes decayed into pairs of neutrinos:

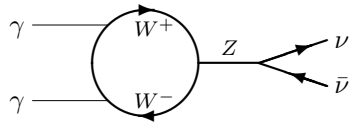

Most of the Z particles did not produce neutrinos, but annihilated back into photons that in repeated collisions produced new Z particles of which a small portion again decayed into neutrinos. In this way more and more heavy neutrinos gradually accumulated as long as the temperature of the universe remained high.

As a result of this process, the bulk of the matter in the universe consists of heavy so-called sterile neutrinos that, like the Higgs, may appear in a continuous mass spectrum.

In an alternative process, photons in head-on collisions produced heavy Higgs particles. Some of them decayed into pairs of Z particles that, instead of annihilating via pairs of charged particles, occasionally produced pairs of stable neutrinos:

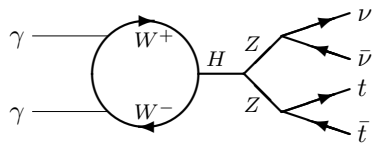

Instead of being products of colliding photons, Higgs particles that give rise to neutrinos may be produced from gluons created in the decay of multiquarks: two-quark mesons, three-quark baryons, tetraquarks, pentaquarks, etc. Since these Higgs particles have well-defined masses — compare with the 750-GeV Higgs discussed in Section 3.6 — their final decay products, the neutrinos, are 25
also expected to appear in well-defined calculable mass states. Consequently, characteristic radiation they occasionally produce in collisions with ordinary matter might reveal their presence in the dark matter.

Due to the expansion of the universe, primordial heavy neutrinos that initially traveled at relativistic speeds have by now lost most of their kinetic energy through redshifting. Thus, a considerable portion of the heavy neutrinos are today moving at a sufficiently slow speed for them to be gravitationally captured in galaxies and galaxy clusters.

4 Cosmological considerations

A maximally simple model (MxSM) of elementary particles describes how an originally unstable matter-antimatter-symmetric universe transforms into a stable matter-dominated world, with protons and electrons bearing its mass. A computer simulation of the evolution of the young universe suggests that it remains in an indefinite quantum state during its first phases.

> The universe of the model begins in the form of a single massive, neutral, and spinless boson. This particle was first described by Paul Dirac in 1971 [24]. The "D particle" may be looked upon as a relativistic harmonic oscillator [25], which is unstable (is its own antiparticle) and may disintegrate into a pair of photons as well as a pair of massive spin-0 bosons [26]. These charged "spinless tauons" are predecessors of today's spin-$\frac{1}{2}$ tauons, which are a kind of superheavy electrons. After its decay, the primordial D particle cannot be recreated (introduction of an electromagnetic field means that the equations defining the particle are no longer consistent [24]), which implies that no trace of it — neither real nor virtual — can be seen today. However, its offspring (the tauon and the tauon's successors, the heavy electron also known as muon and the ordinary electron) bear witness of its existence. The measured tauon–muon and muon–electron mass ratios ($m_\tau/m_\mu = 16.82$ and $m_\mu/m_e = 206.768$, respectively), as well as the observed photon–baryon number ratio (N_γ/N_b) of about 2×10^9, contain information about the universe's early phases. Thanks to this information, a simulation [27] of the evolution of the universe during its first four femtoseconds produces precise unambiguous results — no freely adjustable parameters appear in the computations. Thus, the simulation leads to a theoretical value, 206.768 283 185(78) [28], of the muon–electron mass ratio that is 67 times more precise than the experimentally obtained 2006 CODATA value of 206.768 2823(52).

The simulation predicts that, at the beginning of its present phase, the expanding universe consists of a single proton–antiproton pair at rest in a calm sea of billions of photons, which — being pairwise entangled — form diphoton systems at rest.

The proton–antiproton pair is unstable. However, the law of conservation of momentum, energy, and mass requires the material universe to be preserved, and prevents the two particles of the pair from annihilating each other. Instead, it forces the antiproton to split into an electron and a neutral pion ($\bar{p} \to e^- \pi^0$).

> The intrinsic parities of protons and antiprotons, or, more generally, fermions and antifermions, are positive and negative, respectively. However, the antiproton that carries half of the universe's mass is created with positive parity, which means that it seeks to immediately combine with the proton into a pair of photons. Since the result would be a purely radiative universe and an expanding, non-material universe is forbidden by the law of conservation of energy, the proton–antiproton annihilation is prevented from taking place. Instead, the universe is forced to undergo a quantum

leap from its doomed state to the nearest viable state. This means that the antiproton is forced to split into an electron (e^-) and a neutral pion (π^0) with parity conserved. The neutral pion that inherits the antiproton's positive parity rapidly annihilates into two photons via strong interaction (physical pions have negative intrinsic parity and annihilate slowly through parity-changing weak interaction). The enforced quantum leap of the positive-parity antiproton into an electron and a positive-parity pion must not be confused with proton decay ($p \to e^+\pi^0 \to e^+\gamma\gamma$) and corresponding antiproton decay ($\bar{p} \to e^-\pi^0 \to e^-\gamma\gamma$) predicted by so-called grand unified theories (GUTs).

The appearance of the free non-entangled electron, which carries kinetic energy and charge, and interacts with the background photons, means that the universe exits its initial state of quantum indeterminacy. Thereby, it signals the start of long-range electromagnetic and gravitational interactions between particles.

MxSM is based on the law of conservation of momentum, energy, and mass. The momentum equation — also known as the fundamental hydrodynamic equation — mathematically expresses the law of conservation of momentum. A subset of it may be written in a form that lacks reference to molecules, heat, and pressure. The simplest solution to this "pressureless space equation" suggests that energy creates space, and that the particles within a volume V cause the volume to expand according to $\mathrm{d}V/\mathrm{d}t \propto E$, where E is the total energy of the particles in V [29, p. 44]. It follows that $\mathrm{d}r/\mathrm{d}t \propto r^{-2}E$, where r is the radius of the sphere V. The Hubble expansion rate is defined as $H = \frac{\mathrm{d}r}{\mathrm{d}t}\, r^{-1}$, which means that $H \propto E/r^3$. One may extrapolate the expansion in a relatively small corner of the universe to the entire (in principle visible) universe by setting $\mathrm{d}r/\mathrm{d}t = c$ and $r = R$, which yields $H = c/R$. The radius $R = c/H$ may be said to define the radius of the universe. Since looking out into the universe is equivalent to looking backward in time, R can also be regarded as the distance to the receding "horizon" on which we may imagine seeing the universe come into being. Further, it follows from the momentum equation that the gravitational force appearing in the model is caused by the expansion of the universe, with the strength of the force directly proportional to the Hubble expansion rate. In summary, it holds that $G \propto H \propto Er^{-3}$, where r is the radius of a volume V expanding with the universe and E the total energy of the particles within V. Conservation of energy implies that E is constant, which is a necessary condition for the above-mentioned simulation of the universe's first phases to produce precise testable predictions. 28

Gravity's appearance on the scene signals the start of the universe's final metamorphosis. At this point in time, the universe consists of a proton of mass $m_p = 938.272$ MeV at rest in a sea of $N_\gamma/N_b = 2\,786\,275\,000$ (the initial photon–baryon number ratio) background photons of energy $E_\gamma = 97\,010$ eV [30], two high-energy photons created in the pion decay, and a relativistic electron of mass 0.511 MeV and total energy $E_e = 39.045$ MeV.

For a free particle, it holds that $E^2 = (pc)^2 + (mc^2)^2$, or, setting $c = 1$, $p^2 = E^2 - m^2$. Since the antiproton is at rest, its momentum is zero, and

conservation of momentum implies that $\boldsymbol{p}_e + \boldsymbol{p}_{\pi^0} = \boldsymbol{p}_p = 0$, or $p_e^2 = p_{\pi^0}^2$. Thus, conservation of momentum and energy means that the equations $E_e^2 - m_e^2 = E_{\pi^0}^2 - m_{\pi^0}^2$ and $E_e + E_{\pi^0} = \Delta E$, with $\Delta E = m_p - m_e - m_{\pi^0}$, hold true. Insertion of $E_{\pi^0} = \Delta E - E_e$ into the first of these equations results in $E_e = \frac{1}{2}\Delta E - \frac{1}{2}(m_{\pi^0}^2 - m_e^2)/\Delta E$, which, with $m_p = 938.272$ MeV, $m_{\pi^0} = 134.977$ MeV, and $m_e = 0.511$ MeV, yields $E_e = 39.045$ MeV.

With the proton and background diphotons still being at rest both in the universe and relative to each other, the gravitational pull causes the diphotons to fall toward the proton, which acts as a nucleus of condensation around which a black hole is rapidly formed. The proton at its center gives the newborn primordial black hole (PBH) a positive unit charge.

The picture of black holes painted by MxSM differs radically from the traditional picture according to which particles swallowed by black holes permanently lose their identity. According to MxSM, a black hole is a compact object consisting of densely packed particles hibernating in a frozen, timeless state with their individuality preserved.

It is well known that gravitational time dilation has the effect that — in the eyes of a distant observer — processes of an object falling in toward a black hole appear to slow down until time stops when the object reaches the event horizon.

Inside a black hole, all processes have come to a standstill. Consequently, all forces are inactive, as no exchange of force-mediating gauge particles can occur. Thus, the proton at the center of the PBH comes in the form of three densely packed "deep-frozen" quarks.

The interior of a black hole is a frozen world disconnected from the rest of the universe. This frozen world is revived in a violent explosion if gravity decreases so that the mass of the black hole becomes less than the critical mass,

$$M = \sqrt{\hbar c/G}, \tag{21}$$

which increases with decreasing strength of the gravitational force. Today, $G/\hbar c = 6.708 \times 10^{-39}$ GeV^{-2}, which gives $M = 1.22 \times 10^{19}$ GeV.

Presently, the gravitational force between two electrons is roughly 10^{40} times weaker than the corresponding electromagnetic force. When activated by the exit of the universe from its intial state of quantum indeterminacy, the gravitational force may have been 4.5×10^{31} times stronger than today [30]. This means that, by attracting a small part of the diphotons surrounding it, the proton is able to create a black hole with itself at the center.

Compare the initial critical PBH mass of 1.22×10^{19} GeV$/(4.5 \times 10^{31})^{1/2} = 1.82 \times 10^3$ GeV with the total energy of the photons, $(N_\gamma/N_b)\, E_\gamma = 2\ 786\ 275\ 000 \times 97\ 010$ eV $= 270 \times 10^3$ GeV.

The black hole grows until only about 45 ppm of the photons remain in freedom outside its event horizon [30]. This means that the visible universe undergoes a

rapid "inflation" in which the rate of expansion, H, and gravitational constant, G, decrease by a factor of 0.000 045 and the radius of the universe defined as $R = c/H$ increases by a factor of about 22 000. In other words, when its brief phase of rapid inflation ends, the originally tiny matter-dominated universe with its mass concentrated in a single proton–electron pair has exploded in size and now contains about 10^{13} pairs of positively charged black holes and negatively charged free electrons.

As the universe expands, H and G continue to decrease. According to Eq. (21), the decrease in G causes the critical mass M to increase, with the 30
result that the lightest black holes explode.

> The primordial black holes do not explode all at the same instant because, due to their interaction with the free high-energy electrons and photons, they have acquired slightly differing masses and spin angular momenta. Thus, out of the lightest PBHs, the one with the largest spin should be the first to disintegrate.

The particles ejected in the explosion of a PBH cause a sudden increase in the expansion rate accompanied by an upward jump in the value of G. They provide food for the remaining PBHs, which increase in mass and cause gravity to resume its decrease. Over a period of time, the lightest PBHs are continuously exploding with the remaining PBHs steadily increasing in mass, and gravity decreasing in strength.

During this period, heavy particles are produced in the intense heat of the explosions. Although most of them rapidly annihilate into radiation, some will form stable neutrinos and others long-lived, nearly massless, Higgs particles.

At the beginning of the universe's early epoch characterized by exploding black holes, the repulsive force between PBHs caused by their positive charge outbalances the gravitational attraction between them and keeps them apart. However, sooner or later, a free electron will hit a black hole and merge with it. The resulting neutral PBH will attract neighboring PBHs and together with them form a system of black holes orbiting each other.

Black holes circling each other cause tidal waves on their surfaces, and tear away photons from the crests of the waves until finally the mass of the lightest of the PBHs falls below its critical mass, and the PBH explodes.

As the remaining black holes grow in size, the interaction between them intensifies, and their velocities relative to each other increase. Black holes begin to collide and merge with each other. In these mergers, part of the particles trapped in the PBHs will escape into freedom.

The epoch of decreasing gravity comes to an end when more particles are being released from black holes than are are being captured by them. From now on, the rate of expansion of the universe increases — "the universe accelerates" — and the force of gravity increases in strength.

> More precisely, the gravitational force begins to increase in strength when the energy E (in $G \propto H \propto E/r^3$) grows faster than r^3 (where r is the radius of a volume V expanding with the universe). 29

Today, the rate of expansion of the universe may still be accelerating. However, as the black holes wear down, the acceleration will come to a stop and turn into deceleration. Finally, the universe will return to its original mode of expansion determined by the requirement that $\mathrm{d}V/\mathrm{d}t$ be constant.

Conclusion. MxSM provides precise initial conditions of a black-hole dom- 29
inated universe. These boundary conditions should enable astrophysicists to simulate the evolution of the universe until the present time, and allow them to compare theoretical predictions with actual observations.

In the simulation, one must take into account that the gravitational law of the model differs from Newton's law of gravitation.

> The Newtonian gravitational potential, $U = -Gmr^{-1}$, of a mass m has to be replaced by the gravitational potential
>
> $$U = -Gmr^{-1}(1 - r^2/R^2)^{-1}, \tag{22}$$
>
> which follows from application of the pressureless momentum equation to space [29, p. 13]. Equation (22) implies that, for increasing distances r, the gravitational force $F = M\,\mathrm{d}U/\mathrm{d}r$ between the mass m and another mass M decreases faster than $1/r^2$ and becomes repulsive for $r > R/\sqrt{3}$. As the initially very light black holes increase in mass, they begin to randomly gather into denser "lumps" separated by more sparsely populated "voids". As R increases, the structures bound together by the (over distances $r < R/\sqrt{3}$, attractive) gravitational force grow in size while the same (over distances $r > R/\sqrt{3}$, repulsive) force creates ever vaster voids between the structures. Thus, it appears plausible that structures spanning the presently observable universe may have formed at a time when the bulk of the universe's energy was hidden in black holes and the "radius of visibility", $R = c/H$, was larger than today.

A Higgs lifetime estimates

According to my reference book [16, p. 97], the theoretical decay width for a heavy Higgs boson decaying into pairs of W bosons, Z bosons, and fermions (f) are

$$\Gamma(H \to W^+W^-) = \frac{G_F M_H^3}{8\pi\sqrt{2}} \left(1 - \frac{4M_W^2}{M_H^2}\right)^{1/2} \left(1 - \frac{4M_W^2}{M_H^2} + \frac{12M_W^4}{M_H^4}\right), \quad \text{(A.1)}$$

$$\Gamma(H \to ZZ) = \frac{G_F M_H^3}{16\pi\sqrt{2}} \left(1 - \frac{4M_Z^2}{M_H^2}\right)^{1/2} \left(1 - \frac{4M_Z^2}{M_H^2} + \frac{12M_Z^4}{M_H^4}\right), \quad \text{(A.2)}$$

$$\Gamma(H \to f\bar{f}) = \frac{N_C G_F m_f^2 M_H}{4\pi\sqrt{2}} \left(1 - \frac{4m_f^2}{M_H^2}\right)^{3/2}. \quad \text{(A.3)}$$

N_C in Eq. (A.3) is number of colors. It is 3 for quarks and 1 for the electron. For f denoting a neutrino, $N_C = 0$ because there is no Higgs–neutrino vertex in SM. 4

Even for the observed heavy Higgs particle H_W associated with the W boson, the first two decay modes are excluded because its mass of 125 GeV is less than twice the W and Z masses of $M_W = 80.4$ GeV and $M_Z = 91.19$ GeV, respectively.

Since Higgs–neutrino interactions do not occur, light Higgs particles of mass m_H less than twice the electron mass ($m_H < 2m_e = 1.022$ MeV) do not decay into pairs of massive particles, but will instead annihilate into pairs of photons through electron, down-quark, or up-quark loops.

For Higgs particles annihilating through vacuum-polarization loops, one obtains from Eqs. (A.1) and (A.3) — replacing their trailing parentheses with $(\alpha/2\pi)^2\, x^4$ — to a good approximation

$$\Gamma(H \to W^+W^- \to \gamma\gamma) = \frac{G_F M_H^3}{32\pi\sqrt{2}} \left(\frac{\alpha}{\pi}\right)^2 \quad \text{(A.4)}$$

and

$$\Gamma(H \to f\bar{f} \to \gamma\gamma) = \frac{N_C G_F m_f^2 M_H}{16\pi\sqrt{2}} \left(\frac{\alpha}{\pi}\right)^2 x^4, \quad \text{(A.5)}$$

where $x = -1, -1/3$, or $+2/3$ is the charge in units of e of the electron, down quark, and up quark, respectively. Thus, for the annihilation of a light Higgs particle through a virtual electron, down, or up loop, one arrives at

$$\Gamma(H \to e^+e^- \to \gamma\gamma) = \frac{G_F m_e^2 m_H}{16\pi\sqrt{2}} \left(\frac{\alpha}{\pi}\right)^2, \quad \text{(A.6)}$$

$$\Gamma(H \to d\bar{d} \to \gamma\gamma) = \frac{1}{27} \frac{G_F m_d^2 m_H}{16\pi\sqrt{2}} \left(\frac{\alpha}{\pi}\right)^2, \quad \text{(A.7)}$$

and

$$\Gamma(H \to u\bar{u} \to \gamma\gamma) = \frac{16}{27} \frac{G_F m_u^2 m_H}{16\pi\sqrt{2}} \left(\frac{\alpha}{\pi}\right)^2, \quad \text{(A.8)}$$

respectively.

If, as tentatively concluded in Eq. (6), the masses m_d and m_u appearing squared in Eqs. (A.7) and (A.8) equal the electron mass m_e multiplied by 1/9 and 4/9, respectively, the decay width $\Gamma(H \to u\bar{u} \to \gamma\gamma)$ is $(16/81) \times (16/27) = 0.117$ times the decay width $\Gamma(H \to e^+e^- \to \gamma\gamma)$. This would mean that Higgs particles of mass $m_H < 2m_e = 1.022$ MeV predominantly annihilate through virtual electron loops. 8

For an H_e particle of mass 12 μeV annihilating through an electron loop, one obtains the decay width

$$\begin{aligned}\Gamma(H_e \to e^+e^- \to \gamma\gamma) &= \frac{G_F(\hbar c)^{-3}(m_e c^2)^2}{16\pi\sqrt{2}} \left(\frac{\alpha}{\pi}\right)^2 m_{H_e}c^2 \\ &= 2.7740 \times 10^{-24}\ \text{eV}.\end{aligned} \tag{A.9}$$

With $G_F(\hbar c)^{-3} = 1.166\ 364(5) \times 10^{-5}\ \text{GeV}^{-2}$,
$m_e c^2 = 0.510\ 9989\ \text{MeV} = 0.511 \times 10^{-3}\ \text{GeV}$,
$(\alpha/\pi)^2 = (137.0360 \times 3.141593)^{-2} = 1/185340$,
and $m_{H_e}c^2 = 12 \times 10^{-6}$ eV, 6
one obtains for $\Gamma_{H_e}(e)$ the value
$(1.166364 \times 10^{-5} \times 0.511^2 \times 10^{-6}/71.08613 \times 185340) \times 12 \times 10^{-6}$ eV
$= 3.6547 \times 10^{-17}/13175103$ eV $= 2.7740 \times 10^{-24}$ eV.

The Heisenberg uncertainty principle may be interpreted to mean that the relation $\Delta E \times \Delta t = \hbar$ holds true, or in this case, $\Gamma(H_e) \times \tau(H_e) = \hbar$. With $\hbar = 6.582\ 119 \times 10^{-16}$ eV s, one obtains

$$\tau(H_e \to e^+e^- \to \gamma\gamma) = 2.3728 \times 10^8\ \text{s} = 7.519\ \text{yr} \tag{A.10}$$

for the lifetime of an H_e particle annihilating through a virtual e loop.

$\tau_{H_e}(e) = 6.582119 \times 10^{-16}/2.7740 \times 10^{-24}$ s $= 2.3728 \times 10^8$ s,
or (with 1 yr = 31 556 925.9747 s) $\tau_{H_e}(e) = 7.519$ yr.

B Higgs contribution to the electron mass

In the figure, the propagators for the photon, electron, and Higgs are shown above their corresponding particle lines, while the expressions for the photon–electron and Higgs–electron vertices are shown below the electron line:

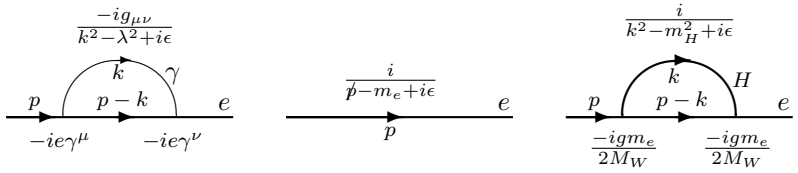

The notation follows the convention established by James Bjorken and Sidney Drell in their book *Relativistic Quantum Mechanics* [31] — the first of their two standard-setting textbooks on quantum field theory (QFT) published in 1964 and 1965, respectively.

Thus, in Feynman's slash notation, $\not{p}$ is the inner product of the four vector γ and the four momentum p, or

$$\not{p} = \gamma \cdot p = \gamma^\mu p_\mu = \gamma_\mu p^\mu, \tag{B.1}$$

where the convention of summing over repeated indices is used (e.g., $\gamma^\mu p_\mu = \gamma^0 p_0 + \gamma^1 p_1 + \gamma^2 p_2 + \gamma^3 p_3$). For the time component of a four vector such as p, it holds that $p^0 = p_0$, and for its space components, $p^i = -p_i$ ($i = 1, 2, 3$). The components p_1, p_2, and p_3 form the momentum vector $\boldsymbol{p}$. The same rules apply to the four vector γ ($\gamma^0 = \gamma_0$ and $\gamma^i = -\gamma_i$ with $(\gamma_1,\ \gamma_2,\ \gamma_3) = \boldsymbol{\gamma}$),

The arrows shown in the figure indicate four momentum — p for the electron, and k for the photon and Higgs. The indices μ and ν indicate that summation over photon and electron polarizations must be performed for the photon–electron loop, while no similar summation is needed for the Higgs–electron loop (the reason for the difference being that the photon is a spin-1 boson and the Higgs a spin-0 boson). For computational reasons, the photon is attributed an infinitesimal mass (λ) that is set equal to zero in final results.

Moving clockwise around the loops and multiplying the expressions with each other, one obtains for the integrand associated with the left (photon–electron) loop,

$$I(\gamma) = \frac{-ig_{\mu\nu}}{k^2 - \lambda^2 + i\epsilon} (-ie\gamma^\nu) \frac{i}{\not{p} - \not{k} - m_e + i\epsilon} (-ie\gamma^\mu), \tag{B.2}$$

and for the integrand associated with the right (Higgs–electron) loop,

$$I(H) = \frac{i}{k^2 - m_H^2 + i\epsilon} \left(-ig\frac{m_e}{2M_W}\right) \frac{i}{\not{p} - \not{k} - m_e + i\epsilon} \left(-ig\frac{m_e}{2M_W}\right). \tag{B.3}$$

The symbol $g_{\mu\nu}$ appearing in the photon propagator is given by the 4×4 matrix (p. 281 in *Relativistic Quantum Mechanics*)

$$g_{\mu\nu} = g^{\mu\nu} = \begin{bmatrix} 1 & & & \\ & -1 & & \\ & & -1 & \\ & & & -1 \end{bmatrix},$$

where only the nonzero elements of the matrix are explicitly shown. Similarly, the components of the four vector γ are the Dirac matrices (p. 282 in the book)

$$\gamma^0 = \begin{bmatrix} 1 & & & \\ & 1 & & \\ & & -1 & \\ & & & -1 \end{bmatrix}, \ \gamma^1 = \begin{bmatrix} & & & 1 \\ & & 1 & \\ & -1 & & \\ -1 & & & \end{bmatrix}, \ \gamma^2 = \begin{bmatrix} & & & -i \\ & & i & \\ & i & & \\ -i & & & \end{bmatrix}, \ \gamma^3 = \begin{bmatrix} & & 1 & \\ & & & -1 \\ -1 & & & \\ & 1 & & \end{bmatrix}.$$

The fundamental property of the γ matrices is the anticommutation relation

$$\gamma^\mu \gamma^\nu + \gamma^\nu \gamma^\mu = 2g^{\mu\nu}, \tag{B.4}$$

that is, $2g^{\mu\nu} I$ with the unit matrix I not explicitly shown.

From (B.4) the rest of the properties of the γ matrices may be derived using the fact that $g_{\mu\nu}$ lowers the index of a four-vector component while $g^{\mu\nu}$ raises it:

$$g_{\mu\nu}\gamma^\nu = \gamma_\mu, \quad g^{\mu\nu}\gamma_\nu = \gamma^\mu, \quad g_{\mu\nu}p^\nu = p_\mu, \quad g^{\mu\nu}p_\nu = p^\mu. \tag{B.5}$$

For instance, multiplication of Eq. (B.4) by $p_\mu q_\nu$ yields

$$\not{p}\not{q} + \not{q}\not{p} = 2p_\mu q^\mu = 2p \cdot q \tag{B.6}$$

(since, being scalar quantities, p_μ and q_ν commute with γ matrices; $\gamma^\nu p^\mu = p^\mu \gamma^\nu$). With $q = p$, this relation simplifies to

$$\not{p}^2 = p^2. \tag{B.7}$$

Also, readily obtained are the relations

$$\gamma_\mu \gamma^\mu = 4, \quad \gamma_\mu \not{p} \gamma^\mu = -2\not{p}, \tag{B.8}$$

the latter via $\gamma_\mu \not{p} \gamma^\mu = \gamma_\mu \gamma_\alpha p^\alpha \gamma^\mu = (2g_{\mu\alpha} - \gamma_\alpha \gamma_\mu)\gamma^\mu p^\alpha = (2\gamma_\alpha - \gamma_\alpha \gamma_\mu \gamma^\mu)p^\alpha = -2\gamma_\alpha p^\alpha$.

Ignoring the infinitesimal constant ϵ, using $g_{\mu\nu}\gamma^\nu = \gamma_\mu$, and introducing the fine-structure constant α and the Fermi coupling constant G_F via the relations

$$e^2 = 4\pi\alpha, \quad G_F/\sqrt{2} = g^2/8M_W^2, \tag{B.9}$$

the integrands may be written

$$I(\gamma) = -4\pi\alpha \frac{\gamma_\mu(\not{p} - \not{k} + m_e)\gamma^\mu}{(k^2 - \lambda^2)((p-k)^2 - m_e^2)} \tag{B.10}$$

and

$$I(H) = \sqrt{2} G_F m_e^2 \frac{\not{p} - \not{k} + m_e}{(k^2 - m_H^2)((p-k)^2 - m_e^2)} \tag{B.11}$$

when the electron propagator is rewritten according to

$$\frac{1}{\not{p} - m_e} = \frac{1}{\not{p} - m_e} \times \frac{\not{p} + m_e}{\not{p} + m_e} = \frac{\not{p} + m_e}{\not{p}^2 - m_e^2} = \frac{\not{p} + m_e}{p^2 - m_e^2}. \tag{B.12}$$

Before the integrands can be weighed against each other, the numerator in Eq. (B.10) must be simplified. With the aid of Eq. (B.8), the integrand becomes

$$I(\gamma) = 8\pi\alpha \frac{\not{p} - \not{k} - 2m_e}{(k^2 - \lambda^2)((p-k)^2 - m_e^2)}. \tag{B.13}$$

Integration over the four momentum k produces a divergent result for k approaching infinity — hence the UV cutoff mass Λ in Eq. (1). The fact that m_H^2 and m_e^2 appear alongside k^2, and m_e alongside k, explains why no particle masses appear in the divergent part of the expression for $\delta m^{(2)}$ (since $m_e/\gamma k$, m_e^2/k^2, and $m_H^2/k^2 \to 0$ for $k \to \infty$).

Division of Eq. (B.11) by Eq. (B.13) shows that in the limit when $k \to \infty$ (and the integral diverges), the ratio between the two integrands is

$$\frac{I(H)}{I(\gamma)} = \frac{G_F m_e^2}{4\sqrt{2}\pi\alpha}. \tag{B.14}$$

References

[1] M. Veltman, *Diagrammatica: The Path to Feynman Diagrams* (Cambridge University Press, 1994).

[2] J. D. Bjorken and S. D. Drell, *Relativistic Quantum Fields* (McGraw-Hill, New York, 1965) pp. 94–96.

[3] K. Johnson, M. Baker, and R. Willey, *Self-Energy of the Electron*, Phys. Rev. **136**, B1111 (1964).

[4] S. Sundman, *On the origin of mass in the standard model*, Int. J. Mod. Phys. E **22** (2013) 1350002, [physicsideas.com/Article.pdf].

[5] S. Sundman, *Resummation of a set of gauge-invariant QED diagrams*, Nucl. Phys. B **656** (2003) 344.

[6] M. Passera, W. J. Marciano, and A. Sirlin, *The muon g – 2 and the bounds on the Higgs boson mass*, Phys. Rev. D **78**, 013009 (2008).

[7] *CODATA recommended values of the physical constants: 2010*, Rev. Mod. Phys. **84**, 1527 (2012), p. 1588.

[8] J. T. Londergan, *Nucleon resonances and quark structure*, Int. J. Mod. Phys. E **18**, 1135 (2009).

[9] W. Greiner, S. Schramm, and E. Stein, *Quantum Chromodynamics*, 2nd ed. (Springer, 2002), pp. 150–151.

[10] Randolf Pohl *et al.*, *The size of the proton*, Nature **466**, 213 (2010).

[11] Evgeny Epelbaum *et al.*, *Structure and Rotations of the Hoyle State*, Phys. Rev. Lett. **109**, 252501 (2012).

[12] John D. Anderson, Philip A. Laing, Eunice L. Lau, Anthony S. Liu, Michael Martin Nieto, and Slava G. Turyshev, *Study of the anomalous acceleration of Pioneer 10 and 11*, Phys. Rev. D **65**, 082004 (2002).

[13] Slava G. Turyshev, Viktor T. Toth, Gary Kinsella, Siu-Chun Lee, Shing M. Lok, Jordan Ellis, *Support for the thermal origin of the Pioneer anomaly*, Phys. Rev. Lett. **108**, 241101 (2012).

[14] *Dictionary of Physics*, 6th ed. (Oxford University Press, 2009).

[15] Jeffrey W. Brosius, Adrian N. Daw, and D. M. Rabin, *Pervasive faint Fe XIX emission from a solar active region observed with EUNIS-13: Evidence for nanoflare heating*, The Astrophysical Journal **790**, 112 (2014), [http://iopscience.iop.org/0004-637X/790/2/112].

[16] P. D. B. Collins, A. D. Martin, and E. J. Squires, *Particle Physics and Cosmology* (John Wiley & Sons, 1989).

[17] J. Jenkins *et al.*, *Additional experimental evidence for a solar influence on nuclear decay rates*, Astroparticle Physics **37**, 81 (2012).

[18] J. Jenkins, *Jere Jenkins's articles on arXiv*, arxiv.org/a/jenkins_j_1.atom.

[19] Bellotti & al, *Search for time modulations in the decay rate of 40K and 232Th*, arXiv:1311.7043 [astro-ph.SR] (2014).

[20] A. T. Yue *et al.*, *Improved Determination of the Neutron Lifetime*, Phys. Rev. Lett. **111**, 222501 (2013).

[21] J. Christopher Howk, Nicolas Lehner, Brian D. Fields, and Grant J. Mathews, *Observation of interstellar lithium in the low-metallicity Small Magellanic Cloud*, Nature **489**, 121 (2012).

[22] J. D. Cockcroft and E. T. S. Walton, *Disintegration of Lithium by Swift Protons*, Nature **129**, 649 (1932).

[23] *The Penguin Dictionary of Physics*, 3rd ed. (Market House Books, 2000).

[24] P. A. M. Dirac, *A positive-energy relativistic wave equation*, Proc. R. Soc. Lond. A322, 435 (1971).

[25] L. C. Biedenharn, M. Y. Han, and H. van Dam, *Generalization and Interpretation of Dirac's Positive-Energy Relativistic Wave Equation*, Phys. Rev. D 8, 1735 (1973).

[26] S. Sundman, *Dirac's particle*, physicsideas.com/Dparticle.pdf (2009).

[27] S. Sundman, *Fortran program simulating the evolution of the universe*, physicsideas.com/Simulation.for (2007–2009).

[28] S. Sundman, *Predictive Cosmology: The Standard Model Revisited*, physicsideas.com (2008).

[29] S. Sundman, *A simple model describing a pure QED universe*, physicsideas.com/Paper.pdf (2009).

[30] S. Sundman, *Errata: A simple model describing a pure QED universe*, physicsideas.com/ErrataV2.pdf (2016).

[31] J. D. Bjorken and S. D. Drell, *Relativistic Quantum Mechanics* (McGraw-Hill, New York, 1964) pp. 162–163.